Simulated magnetocaloric properties of MnCr$_2$O$_4$ spinel

Mahmoud A. Hamad[*]

Physics Department, Faculty of Science, Tanta University, Egypt

Abstract

The magnetocaloric properties of MnCr$_2$O$_4$ spinel have been simulated based on a phenomenological model. The simulation of magnetization as function of temperature is used to explore magnetocaloric properties such as magnetic entropy change, heat capacity change, and relative cooling power. The results imply the prospective application of MnCr$_2$O$_4$ spinel to achieve magnetocaloric effect at cryogenic temperatures (20–60 K) near Curie temperatures (38–44 K). According to the obtained results it is recommended that MnCr$_2$O$_4$ spinel can be used as a promising practical material in the active magnetic regenerator cycle that cools hydrogen gas.

Keywords: magnetocaloric effect, MnCr$_2$O$_4$ spinel, magnetic entropy change

I. Introduction

There is an extensive research about the magnetocaloric effect (MCE) and nowadays the main goal of the MCE study is related to its potential for magnetic refrigeration in the ambient temperature and in cryogenic temperatures [1–5]. Magnetic refrigeration provides a promising solution for cooling [6–11]. It is more efficient, inexpensive, and environmentally friendly than the current refrigerator that uses greenhouse gases [12–19]. Chromites with a formula MCr$_2$O$_4$ (M = Mn, Fe, Co, Ni, Cu) have normal spinel structure with cubic symmetry. According to the spinel structure Mn^{2+} and Cr^{3+} reside at tetrahedral and octahedral sites, respectively, where corners of tetrahedral and octahedral sites are occupied by oxygen atoms [20]. MnCr$_2$O$_4$ orders ferrimagnetically at low temperature in the range 41–51 K [20–23]. In addition, it is found that MCr$_2$O$_4$ composite has a very important effect on the NO$_2$ sensing property for potentiometric sensor [24]. Therefore, there is an increasing interest focused on the investigation of synthesis and properties of MCr$_2$O$_4$ materials.

In this paper, magnetocaloric properties of MnCr$_2$O$_4$ spinel were simulated by phenomenological model. Simulation of magnetization as function of temperature was used to predict magnetocaloric properties at cryogenic temperatures near Curie temperature, such as magnetic entropy change, heat capacity change, temperature change, and relative cooling power.

II. Theoretical considerations

According to the phenomenological model proposed by Hamad [25], magnetization as function of temperature and Curie temperature T_C is presented by:

$$M(T) = \frac{M_i - M_f}{2} \tanh(A(T_C - T)) + BT + C \quad (1)$$

where:

$$A = \frac{2(B - S_C)}{M_i - M_f}$$

$$C = \frac{M_i + M_f}{2} - BT_C$$

and M_i is an initial value of magnetization at ferrimagnetic-paramagnetic transition, M_f is a final value of magnetization at ferrimagnetic-paramagnetic transition (Fig. 1), B is magnetization sensitivity (dM/dT) at ferrimagnetic state before transition, S_C is magnetization sensitivity (dM/dT) at Curie temperature T_C.

Dependence of magnetization as a function of temperature given by the equation of state uniquely determines the Curie temperature T_C. Complete alignment of all electrons spins is possible only at low temperatures. As temperature is raised, magnetization is reduced falling slowly at first and then rapidly until a crit-

---
[*]Corresponding author: tel: +966 530714921,
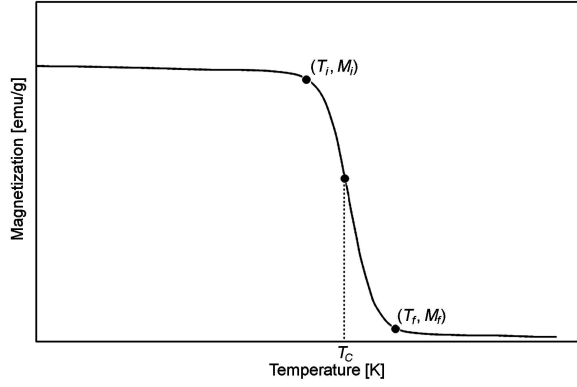e-mail: *m_hamad76@yahoo.com*

Figure 1. Temperature dependence of magnetization under constant applied field

ical temperature T_C is reached. Above T_C, the specimen is no longer ferromagnetic and becomes paramagnetic. Such a cooperative process may be readily understood from thermodynamic reasoning, since the additional entropy associated with disorder of electron spins makes disordered (paramagnetic) state thermodynamically more stable at high temperatures.

A magnetic entropy change of a magnetic system under adiabatic magnetic field shift ΔH from 0 to final value H_{max} is expressed by:

$$\Delta S_M = \left(-A\frac{M_i - M_f}{2}\operatorname{sech}^2(A(T_C - T)) + B\right)H_{max} \quad (2)$$

Therefore, a maximum magnetic entropy change ΔS_{max} (where $T = T_C$) can be assessed with the following equation:

$$\Delta S_{max} = H_{max}\left(-A\frac{M_i - M_f}{2} + B\right) \quad (3)$$

A full-width at half-maximum δT_{FWHM} of magnetic entropy change can be determined by:

$$\delta T_{FWHM} = \frac{2}{A}\cosh^{-1}\left(\sqrt{\frac{2A(M_i - M_f)}{A(M_i - M_f) + 2B}}\right) \quad (4)$$

A magnetic cooling efficiency can be evaluated by considering magnitude of magnetic entropy change (ΔS_M) and its full-width at half-maximum (δT_{FWHM}) [25]. Thus, a relative cooling power (RCP) is calculated by:

$$RCP = -\Delta S_{max} \times \delta T_{FWHM} \quad (5)$$

The magnetization-related change of the specific heat is known [25] and can be expressed by:

$$\Delta C_{P,H} = T\frac{\delta\Delta S_M}{\delta T} \quad (6)$$

According to the phenomenological model [25] $\Delta C_{P,H}$ can be rewritten as:

$$\Delta C_{P,H} = -TA^2(M_i - M_f)\operatorname{sech}^2(\Delta T)\tanh(\Delta T)H_{max} \quad (7)$$

where $\Delta T = A(T_C - T)$. From this phenomenological model, we can simply assess the values of δT_{FWHM}, $|\Delta S|_{max}$ and RCP for MnCr$_2$O$_4$ spinel under different magnetic fields.

III. Results and discussion

Figure 2 shows magnetization of MnCr$_2$O$_4$ spinel versus temperature for different applied magnetic fields. The symbols represent experimental data determined by Mufti *et al.* [23]. The temperature range from 5 to 20 K has not been modelled due to helicoidal transition causing inverse magnetocaloric effect (i.e., a positive entropy change). The dashed curves represent modelled data obtained using model parameters given in Table 1 and equation (1). It can be seen that the calculated results are in a good agreement with the experimental results. In addition, the phenomenological model was used for determination of the changes of magnetic entropy and specific heat as functions of temperature (Figs. 3 and 4), as well as some other important parameters of MnCr$_2$O$_4$ spinel (Table 2).

The magnetic entropy changes of MnCr$_2$O$_4$ spinel are presented in Fig. 3. It is important to stress that this simple phenomenological model is able to predict the peak and plateau observed in the calculated magnetocaloric effect (MCE) curves. The magnetic entropy change data revealed the characteristics spin reorientation by the kinks in the ΔS_M curves. The maxima observed in the $|\Delta S_M|$ curve are associated with a spin reorientation that occurs continuously. The behaviour of this curve suggests how to extend the range of temperatures for use in MCE. The values of maximum magnetic entropy change, full-width at half-maximum, and relative cooling power of MnCr$_2$O$_4$ spinel for different applied magnetic field changes are calculated using eqs. 3–5, respectively, and tabulated in Table 2. Furthermore, the maximum and minimum values of specific heat changes of MnCr$_2$O$_4$ spinel are determined from Fig. 4. Moreover, the variation of applied magnetic field allows tuning of T_C of the system. The tunable T_C makes MnCr$_2$O$_4$ spinel potentially useful for the devel-
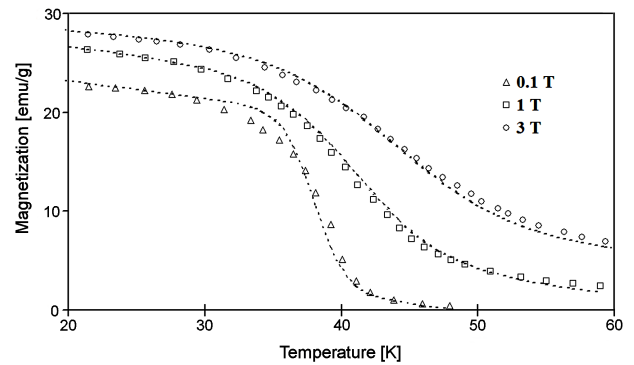

Figure 2. Magnetization of MnCr$_2$O$_4$ spinel versus temperature for different applied magnetic fields (dashed curves - modelled results; symbols - experimental data [23])

Table 1. Model parameters for MnCr$_2$O$_4$ spinel for different applied magnetic fields

H	M_i	M_f	T_C	B	S_C
[T]	[emu/g]	[emu/g]	[K]	[emu/g·K]	[emu/g·K]
0.1	20.1	1.81	38	-0.17	-4.12
1	23.1	4.8	41	-0.17	-1.62
3	25.96	7.41	44	-0.10	-1.15

Table 2. Simulated magnetocaloric properties of MnCr$_2$O$_4$ (maximum magnetic entropy change, ΔS_{max}, full-width at half-maximum, δT_{FWHM}, and relative cooling power, RCP, maximum magnetic entropy change, $\Delta C_{P,H}$) for different applied magnetic fields

H	$-\Delta S_{max}$	δT_{FWHM}	RCP	$\Delta C_{P,H(max)}$	$\Delta C_{P,H(min)}$
[T]	[J/kg·K]	[K]	[J/kg]	[J/kg·K]	[J/kg·K]
0.1	0.41	5.4	2.23	4.79	-4.97
1	1.62	15.2	24.69	6.47	-7.99
3	3.45	21.1	72.91	10.48	-13.73
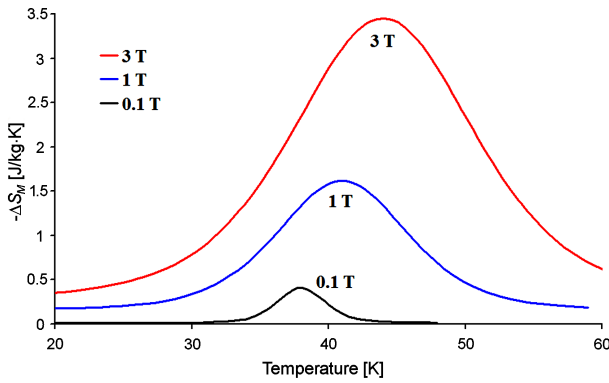
Figure 3. Magnetic entropy change of MnCr$_2$O$_4$ spinel as function of temperature for different applied magnetic fields
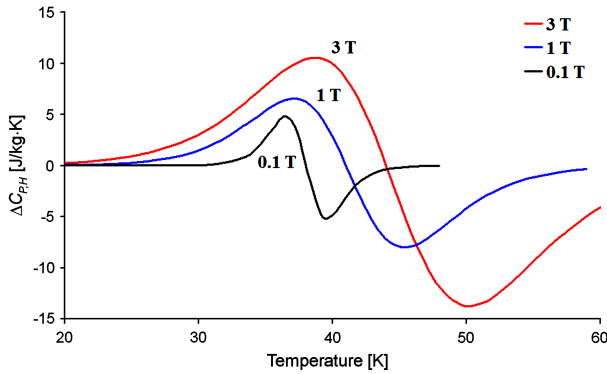
Figure 4. Heat capacity changes of MnCr$_2$O$_4$ spinel as function of temperature for different applied magnetic fields

opment of magnetocaloric regenerators. The largest entropy change value of 3.45 J/kg·K occurs at T = 44 K for ΔH = 3 T with δT_{FWHM} of 21.1 K. The temperature range of the entropy change expanded with increasing magnetic field, i.e. the peaks broaden, which can significantly improve the global efficiency of the magnetic refrigeration. Moreover, the observed uniform distribution of ΔS_M is desirable for an Ericsson-cycle magnetic refrigerator [19].

IV. Conclusions

The phenomenological model allows simulating the temperature dependence of the magnetization of MnCr$_2$O$_4$ spinel under different applied magnetic fields. This allows prediction of magnetocaloric properties of MnCr$_2$O$_4$ spinel such as magnetic entropy change, full-width at half-maximum, relative cooling power, and magnetic specific heat change under different applied magnetic fields. The obtained results indicate on the prospective application of MnCr$_2$O$_4$ spinel due to the observed magnetocaloric effect at cryogenic temperatures near Curie temperatures. Thus, it is recommended that magnetocaloric effect of MnCr$_2$O$_4$ spinel can be used for an apparatus based on the active magnetic regenerator cycle that cools hydrogen gas. Finally, this phenomenological model is more general and can be applied for other data as well as possible applications of MnCr$_2$O$_4$.

References

1. N.A. de Oliveira, P.J. von Ranke, "Theoretical aspects of the magnetocaloric effect", *Phys. Rep.*, **489** (2010) 89–159.
2. K.A. Gschneidner Jr, V.K. Pecharsky, A.O. Tsoko, "Recent developments in magnetocaloric materials", *Rep. Prog. Phys.*, **68** (2005) 1479–1539.
3. M.A. Hamad, "Low magnetic field magnetocaloric effect in Gd$_{5-x}$Eu$_x$Ge$_4$", *J. Supercond. Nov. Magn.*, (2016) DOI: 10.1007/s10948-016-3445-y.
4. L. Li, K. Nishimura, H. Yamane, "Giant reversible magnetocaloric effect in antiferromagnetic GdCo$_2$B$_2$ compound", *Appl. Phys. Lett.*, **94** (2009) 102509
5. X. Bohigas, J. Tajada, E. del Barco, X.X. Zhang, M. Sales, "Tunable magnetocaloric effect in ceramic perovskites", *Appl. Phys. Lett.*, **73** [3] (1998) 390–392.
6. Y. Sun, X. Xu, Y. Zhang, "Large magnetic entropy change in the colossal magnetoresistance material La$_{2/3}$Ca$_{1/3}$MnO$_3$", *J. Magn. Magn. Mater.*, **219** (2000) 183–185.
7. X.X. Zhang, J. Tejada, Y. Xin, G.F. Sun, K.W.

Wong, X. Bohigas, "Magnetocaloric effect in $La_{0.67}Ca_{0.33}MnO$ and $La_{0.60}Y_{0.07}Ca_{0.33}MnO_3$ bulk materials", *Appl. Phys. Lett.*, **69** (1996) 3596–3598.

8. M.H. Phan, S.B. Tian, S.C. Yu, A.N. Ulyanov, "Magnetic and magnetocaloric properties of $La_{0.7}Ca_{0.3-x}Ba_xMnO_3$ compounds", *J. Magn. Magn. Mater.*, **256** (2003) 306–310.

9. M.A. Hamad, "Magnetocaloric effect in Sr_2FeMoO_6/Ag composites", *Process. Appl. Ceram.*, **9** [1] (2015) 11–15.

10. M.H. Phan, S.C. Yu, "Review of the magnetocaloric effect in manganite materials", *J. Magn. Magn. Mater.*, **308** (2007) 325–340.

11. M. Foldeaki, R. Chahine, T.K. Bose, "Magnetic measurements: A powerful tool in magnetic refrigerator design", *J. Appl. Phys.*, **77** (1995) 3528–3537.

12. Y. Xu, U. Memmert, U. Hartmann, "Thermomagnetic properties of ferromagnetic perovskite manganites", *J. Magn. Magn. Mater.*, **242-245** (2002) 698–700.

13. M.A. Hamad, "Magnetocaloric effect in half-metallic double perovskite $Sr_{0.4}Ba_{1.6-x}Sr_xFeMoO_6$", *Int. J. Thermophys.*, **34** (2013) 2144–2151.

14. M.A. Hamad, "Magnetocaloric effect in (001)-oriented MnAs thin film", *J. Supercond. Nov. Magn.*, **27** (2014) 263–267.

15. M.A. Hamad, "Magnetocaloric effect in $Sr_{0.4}Ba_{1.6-x}La_xFeMoO_6$", *J. Supercond. Nov. Magn.*, **27** (2014) 1777–1780.

16. M.A. Hamad, "Simulation of magnetocaloric properties of antiperovskite structural $Ga_{1-x}Al_xCMn_3$", *J. Supercond. Nov. Magn.*, **27** (2014) 2569–2572.

17. M.A. Hamad, "Magnetocaloric effect of perovskite manganites $Ce_{0.67}Sr_{0.33}MnO_3$", *J. Supercond. Nov. Magn.*, **26** (2013) 2981–2984.

18. M.A. Hamad, "Magnetocaloric effect in nanopowders of $Pr_{0.67}Ca_{0.33}Fe_xMn_{1-x}O_3$", *J. Supercond. Nov. Magn.*, **27** (2014) 223–227.

19. M.A. Hamad, "Magnetocaloric effect of perovskite $Eu_{0.5}Sr_{0.5}CoO_3$", *J. Supercond. Nov. Magn.*, **27** (2014) 277–280.

20. E. Winkler, S. Blanco Canosa, F. Rivadulla, M.A. López-Quintela, J. Rivas, A. Caneiro, M.T. Causa, M. Tovar, "Magnetocrystalline interactions in $MnCr_2O_4$ spinel", *Phys. Rev. B*, **80** (2009) 104418.

21. R.N. Bhowmik, R. Ranganathan, R. Nagarajan, "Lattice expansion and noncollinear to collinear ferrimagnetic order in a $MnCr_2O_4$ nanoparticle", *Phys. Rev. B*, **73** (2006) 144413.

22. K. Ohgushi, Y. Kokimoto, T. Ogasawara, S. Miyasaka, Y. Tokura, "Magnetic, optical, and magnetooptical properties of spinel-type ACr_2X_4 (A = Mn, Fe, Co, Cu, Zn, Cd; X = O, S, Se)", *J. Phys. Soc. Jpn.*, **77** (2008) 034713.

23. N. Mufti, G.R. Blake, T.T.M. Palstra, "Magnetodielectric coupling in $MnCr_2O_4$ spinel", *J. Magn. Magn. Mater.*, **321** (2009) 1767–1769.

24. Q. Diao, C. Yin, Y. Guan, X Liang, S Wang, Y Liu, Y. Hu, H. Chen, G. Lu, "The effects of sintering temperature of $MnCr_2O_4$ nanocomposite on the NO_2 sensing property for YSZ-based potentiometric sensor", *Sensors Actuators B: Chem.*, **177** (2013) 397–403.

25. M.A. Hamad, "Prediction of thermomagnetic properties of $La_{0.67}Ca_{0.33}MnO_3$ and $La_{0.67}Sr_{0.33}MnO_3$", *Phase Transitions*, **85** (2012) 106–112.